


Island density scaling in reversible submonolayer growth with attachment barriers

Oliver Smirnov^{1,2,*} and Jacques G. Amar^{1,†}

¹*Department of Physics & Astronomy, University of Toledo, Toledo, Ohio 43606, USA*

²*Department of Physics, Columbia University, New York, New York 10027, USA*

 (Received 6 November 2023; accepted 19 February 2024; published 18 March 2024)

Island nucleation and growth play an important role in thin-film growth. One quantity of particular interest is the exponent χ , which describes the dependence of the saturation island density $N_{\text{sat}} \sim (D_h/F)^{-\chi}$ on the ratio D_h/F of the monomer hopping rate D_h to the deposition rate F . While standard rate equation (RE) theory predicts that $\chi = i/(i+2)$ (where i is the critical island size), more recently it has been predicted that in the presence of a strong barrier to the attachment of monomers to islands, a significantly larger value $\chi = 2i/(i+3)$ may be observed. While this prediction has recently been tested using kinetic Monte Carlo simulations for the case of irreversible growth corresponding to $i = 1$, it has not been tested for the case of reversible island growth corresponding to $i > 1$. Here we present a mean-field self-consistent RE method which we have used to study the dependence of the effective value of χ on D_h/F and barrier-strength for $i = 1, 2, 3$, and 6. Both the no-nucleation-barrier case in which there exists a barrier for monomers to attach to islands larger than the critical island size (but not to smaller islands) and the nucleation-barrier case in which there is a barrier for monomers to attach to islands of all sizes are studied. In all cases, we find that the existence of attachment barriers significantly increases the effective value of χ for a given barrier strength. In addition, for $i = 1$ we find good agreement between our extrapolated asymptotic value of χ and the theoretical strong-barrier prediction both with and without a nucleation barrier. In contrast, for $i > 1$ the value of χ is significantly larger in the presence of a nucleation barrier than in its absence. In particular, while an asymptotic analysis of our results for $i > 1$ also leads to excellent agreement with the strong barrier prediction in the presence of a nucleation barrier, in the absence of a nucleation barrier the asymptotic values are significantly lower.

DOI: [10.1103/PhysRevE.109.034803](https://doi.org/10.1103/PhysRevE.109.034803)

I. INTRODUCTION

Submonolayer island nucleation plays a key role in determining the early stages of thin-film growth. One quantity of particular interest is the exponent χ , which describes the dependence of the saturation island density N_{sat} on the ratio D_h/F of the monomer hopping rate to the deposition rate. In the absence of attachment barriers, corresponding to the diffusion-limited (DL) regime, standard rate equation (RE) theory [1,2] predicts that $N_{\text{sat}} \sim (D_h/F)^{-\chi}$, where the exponent χ is given by the expression [1–3]

$$\chi_{\text{DL}} = \frac{2i}{2i + 2 + d_f}, \quad (1)$$

where i is the critical island size—defined as one less than the number of monomers in the smallest stable island—and d_f is the island fractal dimension. For compact islands ($d_f = 2$), this result implies that $\chi \leq 1$.

However, more recently it has been predicted [4] that in the presence of strong barriers to monomer-island attachment, the exponent χ instead satisfies the attachment-limited expression

(AL) [4]:

$$\chi_{\text{AL}} = \frac{2i}{i + 1 + d_f}. \quad (2)$$

For compact islands ($d_f = 2$), this implies that $\chi > 1$ for $i > 3$. This result is of particular interest since a variety of effects which may lead to attachment barriers have been proposed, including strain and/or electronic effects [5–8], surfactants [9–13], and catalytic effects [14,15], as well as structural and geometric effects [16–25].

While the AL prediction (2) has recently been tested [26] for the case of irreversible growth corresponding to $i = 1$, it has not been tested for the case of reversible island growth corresponding to $i > 1$. This case is of particular interest, since in a variety of experiments [9–11,18] values of χ which are significantly larger than 1 have been obtained. In addition, while the peak value of χ for $i = 1$ was found in Ref. [26] to be significantly larger in the presence of attachment barriers than in their absence, the asymptotic strong-barrier behavior was not determined.

The purpose of this paper is twofold: (1) develop a computationally efficient method that can be used in the case of reversible growth with attachment barriers and (2) use our method to explore the dependence of the asymptotic exponent χ on critical island size and attachment barriers as well as to determine if there is any difference between the cases of a nucleation barrier and no-nucleation barrier. In particular, here

*oliver.smirnov@rockets.utoledo.edu

†jacques.amar@utoledo.edu

we develop and implement a self-consistent mean-field (MF) RE approach which we have used to study the dependence of the effective value of χ (χ_{eff}) on barrier strength, D_h/F , and critical island size for $i = 1, 2, 3$, and 6. To compare our results with the asymptotic strong barrier prediction Eq. (2), we have also determined the dependence of the peak value of χ (χ_{pk}) on barrier strength for each value of the critical island size.

One of the motivations of our MF RE approach is the fact that, due to the existence of significantly increased monomer densities in the presence of attachment barriers (which significantly increases computational time [27]), combined with the decrease in the island density which leads to the requirement of large system sizes to avoid finite-size effects, kinetic Monte Carlo (KMC) simulations of reversible growth with strong attachment barriers and large D_h/F are computationally prohibitive. In contrast, self-consistent RE calculations are significantly faster and have been shown [28,29] to accurately predict the coverage dependence of the monomer and stable island densities in the pre-coalescence regime. In addition, since they are deterministic they do not suffer from statistical fluctuations. Since we are only interested in the stable island density, the use of a MF approach further allows us to enhance the speed of our calculations. To validate our approach, we also present a comparison with full RE results for $i = 1$ as well as with KMC results for $i = 2$.

As in our previous KMC simulations and full RE calculations for the case of irreversible growth [26], we have studied two different cases. In the first case, which we will refer to as the nucleation-barrier case, we assume that there exists a barrier for monomers to attach to other monomers as well as to all islands regardless of their size. In contrast, in the second case, which we will refer to as the no-nucleation-barrier case, there exists a barrier for monomers to attach to stable islands of size $s > i$ (where s is the number of monomers in an island) but not to other monomers or unstable islands of size $s \leq i$. One of the motivations for studying this case is the existence of geometric effects in the case of organic thin-film deposition [17,22], which may lead to a barrier for monomers to attach to stable islands but not to smaller islands. We also present an asymptotic analysis for all values of i for the peak value of χ (χ_∞) in the limit of a very strong attachment barrier.

In all cases, we find that for sufficiently large values of D_h/F , the existence of an attachment barrier significantly increases the effective value of χ for a given barrier strength. In addition, for the case of irreversible growth ($i = 1$), we find good agreement between our extrapolated asymptotic value of χ and the theoretical strong-barrier prediction (2) both with and without a nucleation barrier. In contrast, we find that for $i > 1$, the value of χ is significantly larger in the presence of a nucleation barrier than in its absence. In particular, while an asymptotic analysis of our results for $i > 1$ also leads to excellent agreement with the strong barrier prediction in the presence of a nucleation barrier, in the absence of a nucleation barrier the asymptotic values are significantly lower.

To further understand our results, we have also compared them with the assumptions used in Ref. [4] in deriving Eq. (2). For $i = 1$, we find that these assumptions are valid both with and without a nucleation barrier, thus confirming the good agreement between the two cases. However, for $i > 1$ we find

that—due to the existence of detachment and island attachment barriers—these assumptions do not hold. Surprisingly, despite this, we still find good agreement with the asymptotic prediction for the case of a nucleation barrier.

II. SELF-CONSISTENT MF RE APPROACH

The usual self-consistent RE approach [28–30] involves the numerical integration of the monomer density N_1 as well as the densities N_s of all islands of size s (where s is the number of monomers in an island) as a function of coverage θ . However, since we are not interested in the full island-size distribution, in our MF RE approach we only consider the evolution of the monomer and island densities N_s for $s \leq i$ along with the overall stable island density $N = \sum_{s=i+1}^{\infty} N_s$. In particular, for each value of the critical island-size i , we have numerically integrated the following self-consistent MF REs:

$$\frac{dN_1}{d\theta} = 1 - \theta - N_1 - RN_1/\xi^2 + R \sum_{s=2}^i d_s(1 + \delta_{s,2})N_s, \quad (3)$$

$$\frac{dN_s}{d\theta} = RN_1(\sigma_{s-1}N_{s-1} - \sigma_s N_s) + k_{s-1}N_{s-1} - k_s N_s + R \sum_{s=2}^i (d_{s+1}N_{s+1} - d_s N_s) (2 \leq s \leq i), \quad (4)$$

$$\frac{dN}{d\theta} = N_i(k_i + RN_1\sigma_i). \quad (5)$$

Here $R = D_h/4F$, where D_h is the total hopping rate for a monomer far away from an island while d_s is the relative detachment rate of monomers from islands of size s . The terms with σ_s (σ_1) describe the rate of monomer capture by islands of size s (other monomers) while the terms with k_s (where $k_s = s^{2/d_f}$ [28] and d_f is the fractal dimension of the islands) correspond to the deposition of adatoms directly on islands of size s . The numerical integration of Eqs. (3)–(5) then involves determining self-consistently at each integration step the capture numbers σ_s and monomer capture length ξ .

In previous work involving the full REs and irreversible growth [26], the monomer capture length was given by the expression

$$1/\xi^2 = \sigma_1 N_1 + \sum_{s=1}^{\infty} \sigma_s N_s, \quad (6)$$

where

$$\sigma_s = \frac{(2\pi/\gamma)R_s K_1(R_s/\xi)}{\xi K_0\left(\frac{R_s}{\xi}\right) + l_s K_1\left(\frac{R_s}{\xi}\right)}. \quad (7)$$

Here $\gamma = 1 - \theta + N_1$, $R_s = s^{1/d_f}$ is the radius of an island of size s , and the K_j are modified Bessel functions of order j . The attachment length l_s is related to the barrier strength $P_{\text{barr},s}$ via the expression [30,31]

$$l_s = 1/P_{\text{barr},s} - 1, \quad (8)$$

which is based on the assumption that the rate for a monomer one step away from an island of size s to attach is given

by $D_{\text{att}} = P_{\text{barr},s} D_h / n_h$, where n_h is the number of hopping directions (4 on a square lattice, 6 on a triangular lattice).

In this paper, we continue to use Eqs. (7) and (8) for monomers and islands of size $s \leq i$. In particular, for the case of a nucleation barrier, we set $P_{\text{barr},s} = P_{\text{barr}}$ (with $P_{\text{barr}} \leq 1$) while in the no-nucleation-barrier case, we set $P_{\text{barr},s} = 1$, which implies $l_s = 0$. However, the expression for the monomer capture length ξ is replaced by

$$1/\xi^2 = \sigma_1 N_1 + \sum_{s=1}^i \sigma_s N_s + \sigma_{\text{av}} N \quad (9)$$

while the MF capture number σ_{av} for stable islands is given by

$$\sigma_{\text{av}} = \frac{(2\pi/\gamma) R_{\text{av}} K_1(R_{\text{av}}/\xi)}{\xi K_0\left(\frac{R_{\text{av}}}{\xi}\right) + l_{\text{av}} K_1\left(\frac{R_{\text{av}}}{\xi}\right)}, \quad (10)$$

where $R_{\text{av}} = S_{\text{av}}^{1/d_f}$ is the average stable island radius, $S_{\text{av}} = (\theta - \sum_{s=1}^i s N_s) / N$ is the average stable island size, and $l_{\text{av}} = 1/P_{\text{barr}} - 1$. We note that this expression corresponds to the assumption that the mean capture number of stable islands $\sigma_{\text{mean}} = \frac{1}{N} \sum_{s>i} N_s \sigma_s$ is well approximated by the capture number of an island with the average island-size. Since the island-size distribution is known to be sharply peaked around the average stable island size [32] and the dependence of σ_s on s is relatively weak, this is a reasonable approximation.

Our expressions for the relative detachment rates d_s for unstable islands of size $2 \leq s \leq i$ are the same as derived in Ref. [30],

$$d_s = \frac{\omega_s \sigma_{s-1}}{m_{s-1} P_{\text{barr},s-1}} \quad (11)$$

where ω_s corresponds to the microscopic detachment rate from an island of size s . Here m_s corresponds to the total number of paths for monomers which are one hop away to attach to an island of size s . However, Eq. (8) differs from previous work [30] in which the expression

$$l_s = \frac{2\pi R_s}{P_{\text{barr},s} m_s} - 1 \quad (12)$$

was derived for islands of size s with attachment barriers as well as detachment. In contrast to Ref. [30], this makes our approach consistent with previous work for the case of irreversible growth with [26] and without [28] an attachment barrier for which good agreement with KMC simulations was obtained. We also found that this gave better agreement with KMC simulations for the case $i = 2$ both with and without a barrier.

To study the dependence on critical island-size and attachment barrier, self-consistent MF RE calculations were carried out for $i = 1, 2, 3$, and 6 while the attachment barriers ranged from $P_{\text{barr}} = 1$ (no barrier) to a very strong barrier ($P_{\text{barr}} = 0.001$). In each case, the island-density N_{sat} (corresponding to the stable island density at a coverage $\theta = 0.3$) was determined for values of R ranging from 10^5 to 10^{13} . The effective value of the exponent χ for a given value of R was then calculated using the expression

$$\chi_{\text{eff}}(R) = -\log \left[\frac{N_{\text{sat}}(aR)}{N_{\text{sat}}(R/a)} \right] / \log(a^2), \quad (13)$$

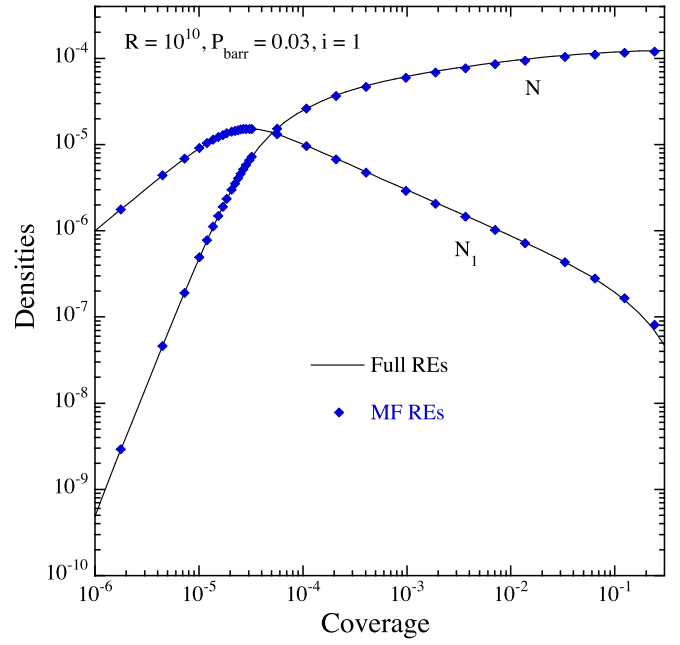


FIG. 1. Comparison between full REs (solid line) [26] and self-consistent MF REs (symbols) for $i = 1$ in the presence of a nucleation barrier. In both RE calculations, $d_f = 1.9$ was assumed.

with $a = 10^{1/4}$. We note that $\chi_{\text{eff}}(R)$ is expected to increase [26,33] with increasing R in the AL regime corresponding to $l_{\text{av}} > l_d$ (where l_d is the average distance between islands) before reaching a peak value $\chi_{\text{pk}} = \chi_{\text{eff}}(R_{\text{pk}})$ when $l_{\text{av}} = l_d$ and then very slowly decreasing towards the DL value as R increases further. Accordingly, for each value of the critical island-size i and detachment rate, the corresponding values of χ_{pk} and R_{pk} were determined as a function of P_{barr} .

III. RESULTS

A. Results for $i = 1$

1. Comparison with full RE calculations

In previous work [26], good agreement was obtained between KMC simulations of irreversible growth on a square lattice ($i = 1$, $d_f \simeq 1.9$) and the full REs. Accordingly, as a first test of our MF REs we have carried out a comparison between our self-consistent MF RE results and those obtained using the full REs. Figure 1 shows a typical comparison between the two for the case $R = 10^{10}$ and $P_{\text{barr}} = 0.03$. As can be seen, there is very good agreement between the MF RE and full RE results for both the island density $N(\theta)$ and monomer density $N_1(\theta)$.

2. Asymptotic behavior for $i = 1$

In previous work for this case [26], the largest value of R studied was 10^{11} , while the smallest value of P_{barr} was 0.01. As a result, the largest value of χ_{pk} obtained in RE calculations and simulations was $\chi_{\text{pk}} \simeq 0.45$. Here, we extend these results using our self-consistent MF RE approach to both larger values of R ($R = 10^{13}$) and stronger attachment barriers. As can be seen in Fig. 2, the highest value of χ_{pk} reached is somewhat larger, e.g., $\chi_{\text{pk}} \simeq 0.47$. We have also used these results to determine the asymptotic (strong barrier) value of

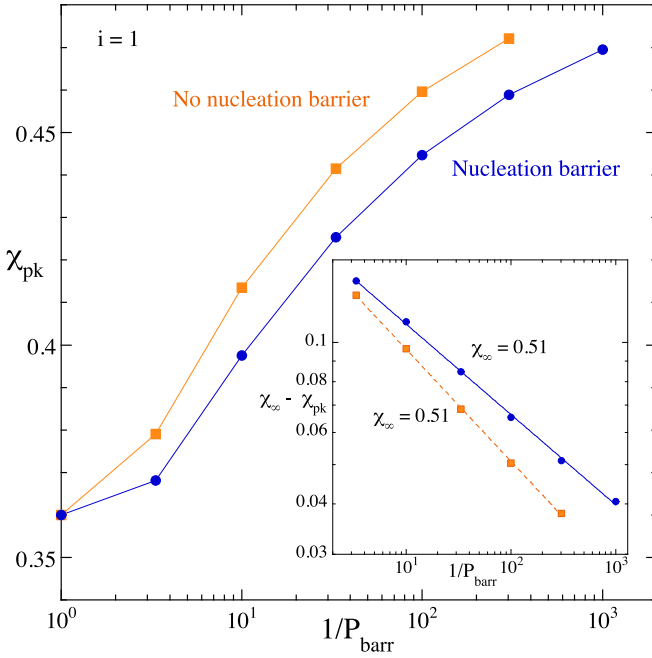


FIG. 2. Self-consistent MF RE results for $\chi_{pk}(1/P_{barr})$ for the case of irreversible growth ($i = 1$, $d_f = 1.9$) both with (filled squares) and without (filled circles) a nucleation barrier. Inset shows corresponding estimates of χ_∞ based on best power-law fits as discussed in text.

$\chi_{pk}(1/P_{barr})$ [e.g., $\chi_{pk}(\infty)$] by assuming that for sufficiently small values of P_{barr} , a plot of $\chi_{pk}(\infty) - \chi_{pk}(1/P_{barr})$ versus $1/P_{barr}$ satisfies a power law. As can be seen from the inset of Fig. 2, using the value $\chi_{AL} = 2i/(i + 1 + d_f) \simeq 0.51$ given by Eq. (2) for $\chi_{pk}(\infty)$, gives an excellent power-law fit for both the case of a nucleation barrier (filled circles) and no nucleation barrier (square symbols). In contrast, either larger or smaller values for $\chi_{pk}(\infty)$ gave much poorer fits. Thus, our results conclusively demonstrate excellent agreement in the asymptotic limit with the theoretical prediction [4] for the case of irreversible growth ($i = 1$) both with and without a nucleation barrier.

B. Results for $i = 2$

1. Comparison between MF REs and full REs ($i = 2$)

To validate our self-consistent MF RE approach for the case of reversible growth with a barrier, we have also carried out KMC simulations for $i = 2$ both with and without nucleation barriers. In this case, we consider a model [29,32] corresponding to growth on a triangular lattice with one-bond detachment (but no detachment if an atom has two or more nearest-neighbor bonds) which implies that the smallest stable island is a compact trimer. As in Refs. [29,32], in our simulations monomers were deposited randomly on an initially empty substrate corresponding to an $L \times L$ triangular lattice with periodic boundary conditions and (per site) deposition rate F . To minimize finite-size effects and improve the statistics, large values of L (typically, $L = 3000$ – 5000) were used. In the absence of a barrier, monomers were assumed to carry out random nearest-neighbor hops with rate $D_h/6$ in each

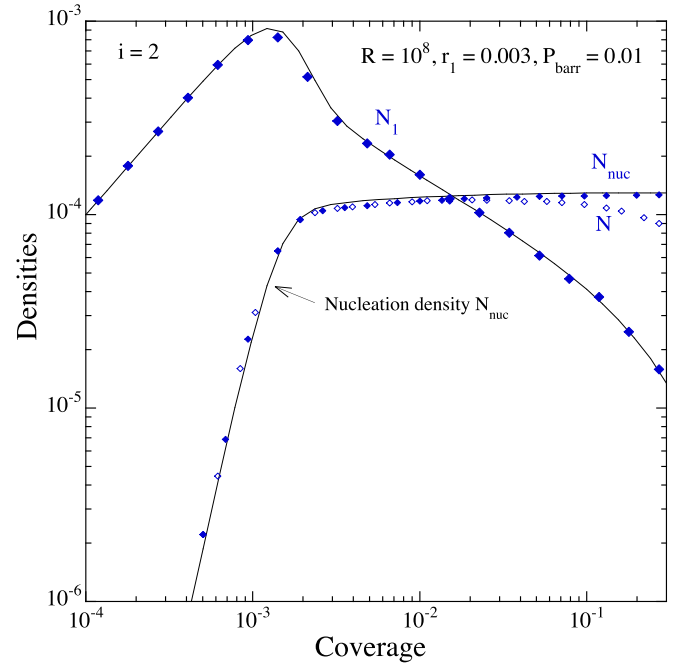


FIG. 3. Comparison between KMC results (symbols) and MF RE results (lines) for $i = 2$ in the presence of nucleation barrier. Small open diamonds correspond to island density including coalescence, while small filled diamonds correspond to nucleation density.

direction. In contrast, in the case of a barrier the hopping rate for a monomer to hop to a site which is nearest neighbor to another occupied site was reduced by a factor of P_{barr} . As previously assumed in Ref. [26], monomers which land on top of another monomer or island were assumed to immediately diffuse to a nearby perimeter site on the substrate.

One-bond edge diffusion with rate $D_e = r_e D_h/6$ (where typically $r_e = 0.01$) was also included to allow edge atoms to rapidly diffuse to stable two-bond sites. To ensure that this does not lead to dimer diffusion, one-bond edge diffusion was suppressed in the case of dimers. For comparison with our KMC simulations—for which the rate of one-bond detachment in each direction was given by $r_1 D_h/6$ —in our REs we assumed $\omega_2 = r_1$, since each of the dimer atoms can detach in three different directions. In agreement with previous work [29], an analysis of the geometry of attachment to monomers indicates that $m_1 = 18$. In addition, due to the existence of one-bond edge diffusion which tends to smooth the islands, as well as the existence of attachment barriers for large islands, we have assumed a value for the island fractal dimension ($d_f = 1.9$), which is somewhat larger than the diffusion-limited attachment [34] value of 1.72. Since our REs do not take into account the effects of coalescence at higher coverage, for comparison with our RE calculations, in our KMC simulations we have also calculated the nucleation density $N_{nuc}(\theta)$, corresponding to the total number of islands (trimers) nucleated, divided by L^2 in addition to the total stable island density N .

Figure 3 shows a typical comparison between KMC simulation results and our self-consistent MF RE results for the case $i = 2$, $R = 10^8$, and $P_{barr} = 0.003$ with a nucleation barrier. As can be seen, there is very good agreement between

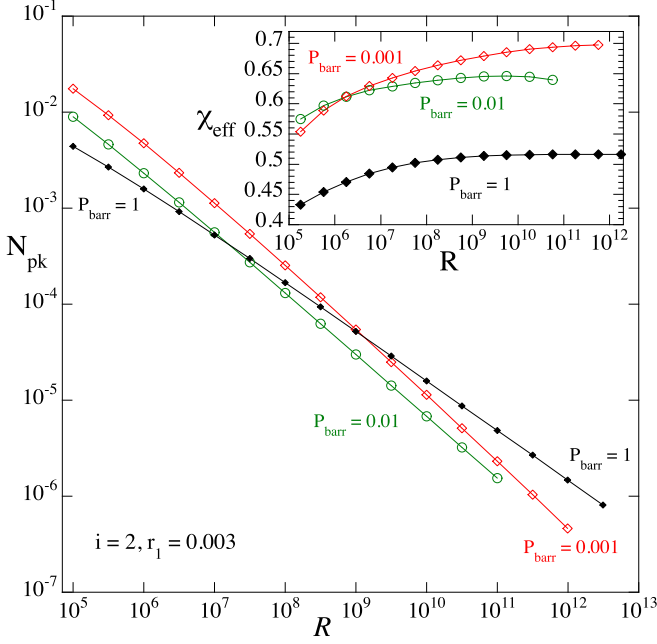


FIG. 4. Self-consistent MF RE results for N_{pk} as function of R for the case of reversible growth ($i = 2$) with nucleation barrier for $r_1 = 0.003$ for $P_{barr} = 0.001, 0.01$, and 1 and $d_f = 1.9$. Inset shows corresponding values of $\chi_{eff}(R)$.

the KMC and MF RE results for both the monomer density $N_1(\theta)$ and the nucleation density $N_{nuc}(\theta)$. Similarly, good agreement has also been obtained for the same parameters with no nucleation barrier (not shown) as well as for the case of no barrier ($P_{barr} = 1$). In addition, as was previously found for the case $i = 1$ [26], there is very little difference between the peak value of N (open diamonds) and the saturation value of N_{nuc} (filled diamonds) obtained from KMC simulations.

2. Dependence of $\chi_{eff}(R)$ on barrier strength for $i = 2$

To study the dependence on detachment rate and barrier, several different possible values for r_1 ($r_1 = 0.003, 0.01$, and $.03$) were considered, while the value of P_{barr} ranged from 0.001 (very strong barrier) to 1 (no barrier). To determine the peak value $\chi_{pk}(P_{barr})$ of $\chi_{eff}(R)$ for each value of P_{barr} , calculations were carried out for values of R ranging from 10^5 to $10^{11} - 10^{13}$, with each value of R separated by a factor of $10^{1/4}$.

Figure 4 shows some typical results for $N_{pk}(R)$ for the case $r_1 = 0.003$ and $P_{barr} = 0.001, 0.01$, and 1 with $d_f = 1.9$. As can be seen, for $P_{barr} = 1$ the corresponding slope and value of $\chi_{eff}(R)$ (see inset) increases with increasing R before saturating at a value $\chi_{pk} \simeq 0.51$ for $R > 10^9$, in good agreement with Eq. (1) assuming $d_f = 1.9$. In contrast, for $P_{barr} = 0.01$, $\chi_{eff}(R)$ increases with increasing R to a somewhat larger peak value $\chi_{pk} \simeq 0.65$ before decreasing with increasing R for $R > 10^{10}$. Finally, for $P_{barr} = 0.001$, $\chi_{eff}(R)$ reaches a peak value $\chi_{pk} \simeq 0.7$ for $R \simeq 10^{11.75}$.

3. Dependence of χ_{pk} on barrier strength for $i = 2$

Figure 5 shows our results for χ_{pk} as a function of $1/P_{barr}$ for all three values of r_1 both with (blue symbols, lines) and

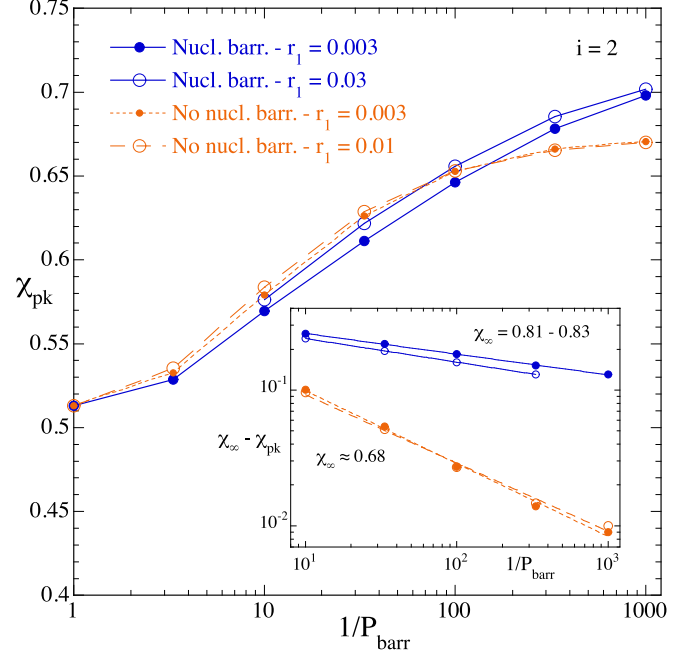


FIG. 5. Self-consistent MF RE results for $\chi_{pk}(P_{barr})$ for the case of reversible growth ($i = 2$) both with and without a nucleation barrier for different values of r_1 and $d_f = 1.9$. Inset shows corresponding estimates of χ_{∞} based on best power-law fits as discussed in text.

without (orange symbols, dashed lines) a nucleation barrier. As can be seen, even for the strongest barrier ($P_{barr} = 0.001$) the values of χ_{pk} for both cases are still lower than the asymptotic theoretical prediction $\chi_{AL} = \frac{2i}{i+1+d_f} \simeq 0.816$ given by Eq. (2) with $i = 2$ and $d_f = 1.9$. In addition, while the values of χ_{pk} with and without a nucleation barrier are very similar for small values of $1/P_{barr}$, for larger values χ_{pk} is significantly larger in the presence of a nucleation barrier.

To determine the asymptotic value of χ_{pk} corresponding to very large $1/P_{barr}$, we again assume that for sufficiently large values of $1/P_{barr}$, the quantity $\chi_{pk}(\infty) - \chi_{pk}(1/P_{barr})$ exhibits a power-law dependence on $1/P_{barr}$. As can be seen from the inset of Fig. 5, using values of $\chi_{pk}(\infty)$ close to the theoretical prediction gives an excellent power-law fit for the case of a nucleation barrier (blue symbols, solid lines). In contrast, using values for $\chi_{pk}(\infty)$ which are larger or smaller than this value gave much poorer fits. Thus, our results indicate that in the presence of a nucleation barrier, the asymptotic value of χ_{eff} agrees with the theoretical prediction Eq. (2). In contrast, for the case of no nucleation barrier (orange symbols, dashed lines) we find that the best power-law fit corresponds to a significantly smaller asymptotic value, e.g., $\chi_{\infty} = 0.68$. This is in contrast to Ref. [4], which indicates that there should be no difference between the two cases.

C. Results for $i = 3$

In this case, we considered a model [29,32] corresponding to growth on a square lattice with one-bond detachment and fast edge and corner diffusion, which implies that islands are compact ($d_f = 2$) while the smallest stable island is a

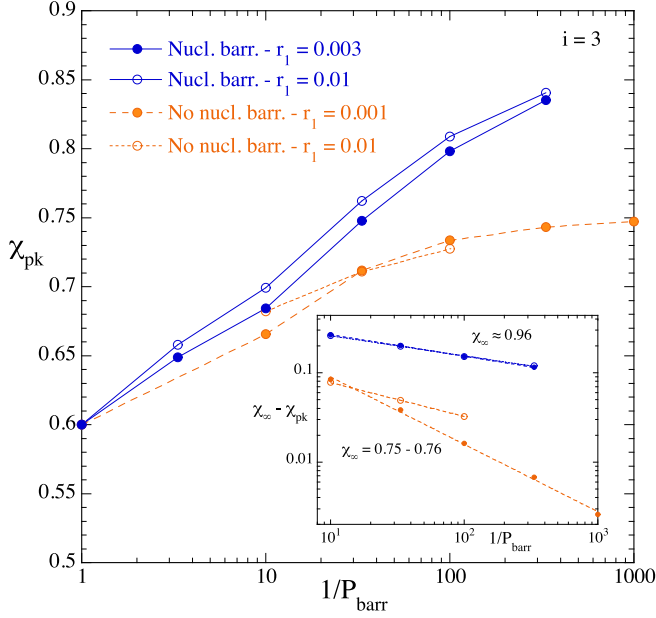


FIG. 6. Self-consistent MF RE results for $\chi_{\text{pk}}(1/P_{\text{barr}})$ for $i = 3$ both with and without a nucleation barrier for different values of r_1 . Inset shows corresponding estimates of χ_{∞} based on best power-law fits as discussed in text.

tetramer. In particular, we assume that both dimers and trimers are unstable, while the rate of one-bond detachment in a given direction is equal to $r_1 D_h/4$. The corresponding detachment terms in the REs are $\omega_2 = (3/2)r_1$ (since each of the two dimer atoms can detach in three different directions) and $\omega_3 = (5/4)r_1$ (corresponding to an average over the linear and L-shaped trimer cases). An analysis of the attachment geometry for monomers and dimers on a square lattice leads to the values $m_1 = 12$ as in Ref. [29] and $m_2 = 14$. As for the case $i = 2$, several different possible values for r_1 ($r_1 = 0.001, 0.003$, and 0.01) were considered, while the values of P_{barr} again ranged from 0.001 (very strong barrier) to 1 (no barrier). To determine the peak value $\chi_{\text{pk}}(P_{\text{barr}})$ of $\chi_{\text{eff}}(R)$ for each value of P_{barr} , calculations were carried out for values of R ranging from 10^5 to 10^{13} .

Figure 6 shows the dependence of χ_{pk} on P_{barr} for all three values of r_1 both with (blue symbols, lines) and without (orange symbols, dashed lines) a nucleation barrier. We note that in this case the theoretical prediction in the absence of an attachment barrier is $\chi = 3/5$ while in the presence of a strong barrier the prediction is that $\chi = 1$ [see Eq. (2)]. As for the case $i = 2$, the value of χ_{pk} increases with increasing barrier-strength $1/P_{\text{barr}}$ while the corresponding values exhibit very little dependence on the detachment rate r_1 . Similarly, while there is very little dependence on the presence or absence of a nucleation barrier for small values of $1/P_{\text{barr}}$, for larger values the value of χ_{pk} is significantly larger in the presence of a nucleation barrier than in its absence.

As shown in the inset of Fig. 6, to determine the asymptotic value of χ corresponding to very strong attachment barriers we have carried out an asymptotic analysis similar to that used for the case $i = 2$. For the case of a nucleation barrier and all values of the detachment rate r_1 , the asymptotic value of

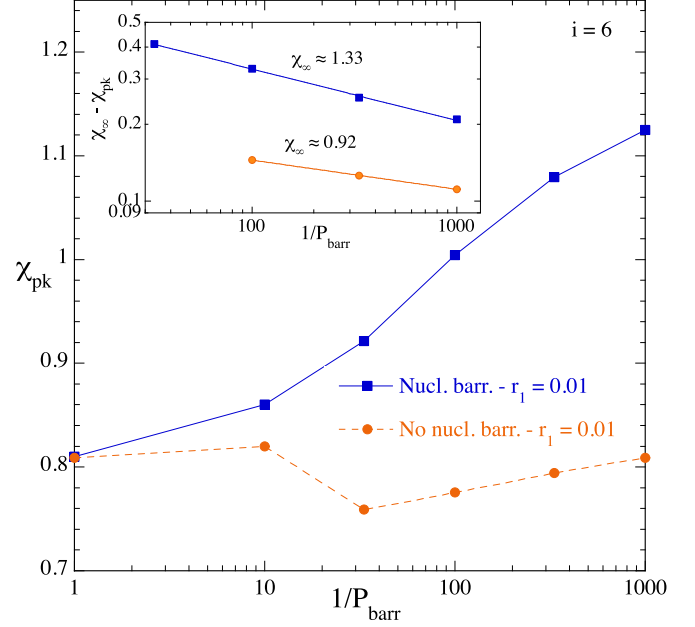


FIG. 7. Self-consistent MF RE results for $\chi_{\text{pk}}(1/P_{\text{barr}})$ for $i = 6$ both with and without a nucleation barrier for $r_1 = 0.01$. Inset shows corresponding estimates of χ_{∞} based on best power-law fits as discussed in text.

χ_{∞} corresponding to the best fit (e.g., $\chi_{\infty} \simeq 0.96$) is in very good agreement with the theoretical prediction $\chi_{\text{AL}} = 1$. On the other hand, for the case of no nucleation barrier the best fit values of χ_{∞} for both values of r_1 (e.g., $\chi_{\infty} \simeq 0.75 - 0.76$) are significantly smaller.

D. Results for $i = 6$

In this case, we considered a model corresponding to growth on a triangular lattice with one-bond and two-bond detachment which implies that the smallest stable island is a compact hexagonal heptamer. We also assume that all stable islands are compact ($d_f = 2$). As for the case $i = 2$, the microscopic rate of dimer detachment was assumed to be given by $\omega_2 = r_1$. While all islands of size $s > 6$ were assumed to be stable, in this case we also took into account the existence of two-bond detachment from trimers, tetramers, pentamers, and hexamers, with relative rates given by $\omega_3 = \omega_4 = r_2$, and $\omega_5 = \omega_6 = 2r_2/3$, where $r_2 = r_1^2$. As for the case $i = 2$, $m_1 = 18$ while we assumed that $m_s = 18 + 4s$ for $s = 2 - 6$. Due to the extensive computational time required, in this case only one value of r_1 ($r_1 = 0.01$) was considered while the values of P_{barr} again ranged from 0.001 (very strong barrier) to 1 (no barrier).

Figure 7 shows our results for χ_{pk} as a function of $1/P_{\text{barr}}$ for both the case of a nucleation barrier (blue symbols, lines) and without a nucleation barrier (orange symbols, dashed lines). We note that in this case the theoretical prediction in the absence of an attachment barrier is $\chi_{\text{DL}} = 3/4$ while the strong barrier prediction is $\chi_{\text{AL}} = 4/3$ [see Eq. (2)]. As can be seen in Fig. 7, for the case of a nucleation barrier the largest value of χ_{pk} (corresponding to $1/P_{\text{barr}} = 10^3$) is approximately equal to 1.1 and is still increasing with increasing

barrier strength. In contrast, for $1/P_{\text{barr}} \geq 10$ the values of χ_{pk} are significantly lower in the absence of a nucleation barrier.

The inset of Fig. 7 shows the corresponding asymptotic analysis. As can be seen, for the case of a nucleation barrier the asymptotic value of χ_{pk} (e.g., $\chi_{\infty} = 1.33$) is in excellent agreement with the theoretical prediction. In contrast, in the absence of a nucleation barrier, the best asymptotic fit leads to a value ($\chi_{\infty} \simeq 0.92$) which is significantly smaller.

IV. CONCLUSION

We have used a MF RE approach to study the dependence of the effective values of $\chi_{\text{eff}}(R)$ on R and barrier strength P_{barr} and critical island-size i for $i = 1, 2, 3$, and 6. In addition, for each value of i we have studied two different cases—one in which there is a barrier for monomers to attach to unstable islands (nucleation barrier) and stable islands, and the other with attachment barriers to stable islands only (no nucleation barrier). For each value of the critical island size and P_{barr} , we have also determined the peak values of $\chi_{\text{eff}}(R)$, e.g., $\chi_{\text{pk}}(1/P_{\text{barr}})$. An asymptotic analysis was then carried out to determine the value of $\chi_{\text{pk}}(\infty)$ in the limit of infinitely strong attachment barriers. For $i = 2$ and $i = 3$, calculations were carried out for several different detachment rates.

As previously found for the case of irreversible growth [26], in the case of reversible growth we find that attachment barriers lead to values of $\chi_{\text{pk}}(1/P_{\text{barr}})$ which are significantly larger than in the absence of an attachment barrier. In addition, for moderate attachment barriers, the presence or absence of a nucleation barrier has relatively little effect on the value of $\chi_{\text{pk}}(1/P_{\text{barr}})$. In contrast, for strong attachment barriers and $i > 1$, we find that $\chi_{\text{pk}}(1/P_{\text{barr}})$ is significantly larger in the presence of nucleation barriers than in their absence, while this difference increases with increasing critical island size. This result is quite surprising, since according to standard theoretical RE analyses [4,35] there should be no difference between the two cases, since only the effect of attachment barriers to stable islands are taken into account.

To further compare with theoretical predictions, we have also carried out an asymptotic analysis of the value of $\chi_{\text{pk}}(1/P_{\text{barr}})$ in the limit of very strong (infinite) barrier. For the case of irreversible growth ($i = 1$), we find good agreement between our extrapolated asymptotic value of $\chi_{\text{pk}}(1/P_{\text{barr}})$ and the theoretical strong-barrier prediction Eq. (2) both with and without a nucleation barrier. In contrast, for the case of reversible growth ($i > 1$), we only find good agreement between the extrapolated asymptotic values of $\chi_{\text{pk}}(1/P_{\text{barr}})$ and the theoretical strong-barrier prediction in the presence of a nucleation barrier, while in the absence of a nucleation barrier, the corresponding asymptotic values are significantly smaller.

To try to understand this discrepancy for the case of reversible island growth, we have examined the validity of some of the assumptions used in standard RE scaling theory [1,2,4]. As shown in Fig. 1, in the case of irreversible growth ($i = 1$), we find that in the standard RE theory assumption that $N_1 \ll N$ in the nucleation regime holds both with and without nucleation barriers. This explains the good agreement between the asymptotic value of χ and the prediction of Eq. (2) in both cases. However, in the case of reversible growth with attachment barriers, this assumption does not hold, as can be seen in Fig. 3 for $i = 2$. Similar results have been obtained (not shown) for $i = 2$ in the absence of a nucleation barrier as well as for $i = 3$ and $i = 6$ both with and without a nucleation barrier. These results imply that for $i > 1$ the dominant contribution to the coverage in the nucleation regime is the monomer density N_1 rather than the stable island density N as was assumed in Ref. [4].

It is also interesting to consider the quantity $G = (1/P_{\text{barr}} - 1)\sqrt{N} \sim l_{\text{av}}/l_d$ [4], which is expected to be much larger than 1 in the AL regime. As expected, for the case of irreversible growth ($i = 1$), we find that $G \gg 1$ for large values of $1/P_{\text{barr}}$ and R both with and without a nucleation barrier. However, for the case of reversible growth with $i = 2, 3$, and 6 the values of G corresponding to χ_{pk} are typically less than 1 both with and without nucleation barriers. Surprisingly, the value of G is actually smaller in the presence of nucleation barriers than in their absence despite the fact that in the former case we find good agreement in the asymptotic limit with Eq. (2). Unfortunately, since the standard RE assumption that $N_1 \ll N$ in the nucleation regime does not hold in this case, we have been unable to provide an analytical explanation for this discrepancy.

In conclusion, we have demonstrated that for both irreversible and reversible growth, and in the presence of a nucleation barrier, the asymptotic value of the strong-barrier exponent χ is in good agreement with the AL expression (2). Similarly, we also find good agreement between our asymptotic results and the AL prediction for χ in the case of irreversible growth without a nucleation barrier. However, in the case of reversible growth without a nucleation barrier, both the effective and asymptotic values of χ are significantly smaller. Further work is needed to understand this discrepancy.

ACKNOWLEDGMENTS

The authors gratefully acknowledge funding support from the NSF Research Experience for Undergraduates (REU) program, Grant No. 1950785 at the University of Toledo. We would also like to acknowledge a grant of computer time from the Ohio Supercomputer Center.

- [1] J. A. Venables, *Philos. Mag.* **27**, 697 (1973).
- [2] J. A. Venables, G. D. Spiller, and M. Hanbucken, *Rep. Prog. Phys.* **47**, 399 (1984).
- [3] M. Schroeder and D. E. Wolf, *Phys. Rev. Lett.* **74**, 2062 (1995).

- [4] D. Kandel, *Phys. Rev. Lett.* **78**, 499 (1997).
- [5] J. Repp, F. Moresco, G. Meyer, K. H. Rieder, P. Hyldgaard, and M. Persson, *Phys. Rev. Lett.* **85**, 2981 (2000).
- [6] N. Knorr, H. Brune, M. Epple, A. Hirstein, M. A. Schneider, and K. Kern, *Phys. Rev. B* **65**, 115420 (2002).

- [7] K. A. Fichtorn, M. L. Merrick, and M. Scheffler, *Phys. Rev. B* **68**, 041404(R) (2003).
- [8] S. M. Binz, M. Hupalo, X. Liu, C. Z. Wang, W.-C. Lu, P. A. Thiel, K. M. Ho, E. H. Conrad, and M. C. Tringides, *Phys. Rev. Lett.* **109**, 026103 (2012).
- [9] B. Voigtländer and A. Zinner, *Surf. Sci. Lett.* **292**, L775 (1993).
- [10] B. Voigtländer, A. Zinner, T. Weber, and H. P. Bonzel, *Phys. Rev. B* **51**, 7583 (1995).
- [11] L. Andersohn, Th. Berke, U. Köhler, and B. Voigtländer, *J. Vac. Sci. Technol. A* **14**, 312 (1996).
- [12] D. Kandel and E. Kaxiras, *Phys. Rev. Lett.* **75**, 2742 (1995).
- [13] E. Kaxiras, *Thin Solid Films* **272**, 386 (1996).
- [14] S. Kosolobov, G. Nazarikov, S. Sitnikov, I. Pshenichnyuk, L. Fedina, and A. Latyshev, *Surf. Sci.* **687**, 25 (2019).
- [15] A. S. Mitko, D. R. Streltsov, P. V. Dmitryakov, A. A. Nesmelov, A. I. Buzin, and S. N. Chvalun, *Polymer Science* **61**, 555 (2019).
- [16] G. Eres, J. Z. Tischler, C. M. Rouleau, H. N. Lee, H. M. Christen, P. Zschack, and B. C. Larson, *Phys. Rev. Lett.* **117**, 206102 (2016).
- [17] T. Potocar, S. Lorbek, D. Nabok, Q. Shen, L. Tumbek, G. Hlawacek, P. Puschnig, C. Ambrosch-Draxl, C. Teichert, and A. Winkler, *Phys. Rev. B* **83**, 075423 (2011).
- [18] L. Tumbek and A. Winkler, *Surf. Sci. Lett.* **606**, L55 (2012).
- [19] D. I. Rogilo, L. I. Fedina, S. S. Kosolobov, B. S. Rangelov, and A. V. Latyshev, *Phys. Rev. Lett.* **111**, 036105 (2013).
- [20] A. Pimpinelli, L. Tumbek, and J. P. A. Winkler, *J. Phys. Chem. Lett.* **5**, 995 (2014).
- [21] D. I. Rogilo, L. I. Fedina, S. S. Kosolobov, and A. V. Latyshev, *Surf. Sci.* **667**, 1 (2018).
- [22] O. Roscioni, G. D'Avino, and L. Muccioli, *J. Phys. Chem. Lett.* **9**, 6900 (2018).
- [23] A. Choukourov, I. Melnichuk, I. Gordeev, D. Nikitin, R. Tafichuk, P. Pleskunov, J. Hanuš, J. Houška, T. Kretková, and M. Dopita, *Prog. Org. Coat.* **143**, 105630 (2020).
- [24] A. S. Petrov, D. I. Rogilo, D. V. Sheglov, and A. V. Latyshev, *J. Cryst. Growth* **531**, 125347 (2020).
- [25] C. Y. Fong, M. D. Watson, L. H. Yang, and S. Ciraci, *Modelling Simul. Mater. Sci. Eng.* **10**, R61 (2002).
- [26] S. Hamadna, I. Khatri, E. H. Sabbar, and J. G. Amar, *Surf. Sci.* **715**, 121938 (2022).
- [27] As an example, the KMC simulation results shown in Fig. 3 ($i = 2$, $R = 10^8$, $r_1 = 0.003$, and $P_{\text{barr}} = 0.01$) took approximately 13 times longer than the equivalent simulation without an attachment barrier while for $P_{\text{barr}} = 0.001$ the equivalent simulation took 81 times longer.
- [28] G. S. Bales and D. C. Chrzan, *Phys. Rev. B* **50**, 6057 (1994).
- [29] M. N. Popescu, J. G. Amar, and F. Family, *Phys. Rev. B* **58**, 1613 (1998).
- [30] G. S. Bales and A. Zangwill, *Phys. Rev. B* **55**, R1973(R) (1997).
- [31] P. Politi and J. Villain, *Phys. Rev. B* **54**, 5114 (1996).
- [32] J. G. Amar and F. Family, *Phys. Rev. Lett.* **74**, 2066 (1995).
- [33] D. L. Gonzalez, A. Pimpinelli, and T. L. Einstein, *Phys. Rev. E* **96**, 012804 (2017).
- [34] T. A. Witten and L. M. Sander, *Phys. Rev. Lett.* **47**, 1400 (1981).
- [35] J. A. Venables and H. Brune, *Phys. Rev. B* **66**, 195404 (2002).